Microbial network, phylogenetic diversity and community membership in the active layer across a permafrost thaw gradient

Journal:	*Environmental Microbiology and Environmental Microbiology Reports*
Manuscript ID	Draft
Journal:	Environmental Microbiology
Manuscript Type:	EMI - Research article
Date Submitted by the Author:	n/a
Complete List of Authors:	Mondav, Rhiannon; Uppsala University, Ecology and Genetics, Limnology; University of Queensland, Chemistry and Molecular Biosciences McCalley, Carmody; Rochester Institute of Technology, Thomas H. Gosnell School of Life Sciences; University of New Hampshire, Earth Systems Research Center Hodgkins, Suzanne ; Florida State University , Department of Earth Ocean and Atmospheric Science Frolking, Steve ; University of New Hampshire, Institute for the Study of Earth, Oceans, and Space Saleska, Scott; University of Arizona, Ecology and Evolutionary Biology Rich, Virginia; University of Arizona, Department of Soil, Water and Environmental Science; Ohio State University, Microbiology Department Chanton, Jeff; Florida State University , Department of Earth Ocean and Atmospheric Science Crill, Patrick; Stockholm University, Department of Geological Sciences
Keywords:	microbial ecology, microbially-influenced global change, environmental signal/stress responses, microbial communities

Microbial network, phylogenetic diversity and community membership in the active layer across a permafrost thaw gradient

Authors:

Rhiannon Mondav[1,2*], Carmody K McCalley[3,4,+], Suzanne B Hodgkins[5], Steve Frolking[4], Scott R Saleska[3], Virginia I Rich[6,^], Jeff P Chanton[5], Patrick M Crill[7]

Affiliations:

[1] Department of Ecology and Genetics, Limnology, Uppsala University, Uppsala 75236, Sweden

[2] School of Chemistry and Molecular Biosciences, University of Queensland, Brisbane 4072, Australia

[3] Department of Ecology and Evolutionary Biology, University of Arizona, Tucson 85721, USA

[4] Institute for the Study of Earth, Oceans, and Space, University of New Hampshire, Durham NH 03824, USA

[5] Department of Earth Ocean and Atmospheric Science, Florida State University, Tallahassee 32306-4320, USA

[6] Department of Soil, Water and Environmental Science, University of Arizona, Tucson 85721, USA

[7] Department of Geology and Geochemistry, Stockholm University, Stockholm 10691, Sweden

*Corresponding author:

RMondav, Norbyvagen, Uppsala University, Uppsala, SE75236 Sweden, +46 (0)7 2731 7286, rhiannon.mondav@ebc.uu.se

Running Title: Microbial community across a permafrost thaw gradient

Current addresses: [+] Thomas H. Gosnell School of Life Sciences, Rochester Institute of Technology, Rochester, New York 14623, USA; [^] Department of Microbiology, The Ohio State University, Columbus 43210, USA.

Summary

Biogenic production and release of methane (CH_4) from thawing permafrost has the potential to be a strong source of radiative forcing. We investigated changes in the active layer microbial community of three sites representative of distinct permafrost thaw stages at a palsa mire in northern Sweden. The palsa sites with intact permafrost, and low radiative forcing signature had a phylogenetically clustered community dominated by *Acidobacteria* and *Proteobacteria*. The bog with thawing permafrost and low radiative forcing signature was dominated by hydrogenotrophic methanogens and *Acidobacteria*, had lower alpha diversity, and midrange phylogenetic clustering, characteristic of ecosystem disturbance affecting habitat filtering, shifting from palsa-like to fen-like at the waterline. The fen had no underlying permafrost, and the highest alpha, beta and phylogenetic diversity, was dominated by *Proteobacteria* and *Euryarchaeota*, and was significantly enriched in methanogens. The mire microbial network was modular with module cores consisting of clusters of *Acidobacteria*, *Euryarchaeota*, or *Xanthomonodales*. Loss of underlying permafrost with associated hydrological shifts correlated to changes in microbial composition, alpha, beta, and phylogenetic diversity associated with a higher radiative forcing signature. These results support the complex role of microbial interactions in mediating carbon budget changes and climate feedback in response to climate forcing.

Introduction

Modern discontinuous permafrost is found in regions with a mean annual air temperature between -5 °C and +2 °C and where the insulating properties of peat enable persistence of permafrost above freezing temperatures (Shur and Jorgenson, 2007; Seppälä, 2011). As these regions experience climate change-induced warming, they are approaching temperatures that are destabilizing permafrost (Schuur et al., 2015). Permafrost degradation typically leads to significant loss of soil

carbon (C) through erosion, fire and microbial mineralisation (Osterkamp et al., 2009; Mack et al., 2011). The area of permafrost at risk of thaw in the next century has been estimated to be between 10^6 and 10^7 km^2, with the quantity of C potentially lost ranging from 1-4 x 10^{14} kg (McGuire et al., 2010; Schuur et al., 2015). Increasing plant production in thawed systems may partially compensate for this loss but this is poorly defined (Hicks Pries et al., 2013). Thus, the potential positive feedbacks to climate change are not well constrained, and will vary depending on the emission ratio of the greenhouse gases (GHGs) carbon dioxide (CO_2) and methane (CH_4), and the time scale considered (Dorrepaal et al., 2009; Nazaries et al., 2013). Changes in microbial community membership (e.g. methanogen to methanotroph ratio) will be a significant factor controlling the CO_2 to CH_4 emission ratio (Hodgkins et al., 2014).

To examine the relationship between permafrost thaw, shifting GHG emissions, and the microbial community, we investigated a natural *in situ* thaw gradient at Stordalen Mire, northern Sweden, on the margin of the discontinuous permafrost zone. Permafrost thaw has been causatively linked to changes in topography, vegetation, and GHG emission at Stordalen (Christensen, 2004; Johansson et al., 2006; Bäckstrand et al., 2008, 2010; Johansson and Åkerman, 2008), and elsewhere (Turetsky et al., 2007; Olefeldt et al., 2013). Currently, the Mire is a partially degraded complex of elevated, drained hummocks (palsas with intact permafrost) and wet depressions (bogs with thinning permafrost and fens without any permanently frozen ground), each representing different stages of thaw (Fig S1), and each characterised by distinct vegetation (Bhiry and Robert, 2006; Johansson et al., 2006). Changes in topography and vegetation (proxy for thaw) have been tracked through the last 40 years and show a decrease in area covered by palsa, an expansion of fens and a variable area covered by bogs (Christensen et al., 2004; Malmer et al., 2005; Johansson et al., 2006). Part of the known palsa-cycle is the external carving and internal collapse of palsas into the surrounding bog or fen, though the time scale at which this happens varies depending on whether dome-

palsas or palsa-complexes/plateaus (as seen at Stordalen) are considered (Railton and Sparling, 1973; Zoltai, 1993; Sollid and Sørbel, 1998; Gurney, 2001; Turetsky et al., 2007; Seppälä, 2011; O'Donnell et al., 2012; Liebner et al., 2015). At Stordalen complete collapse due to absence of permafrost results in a fen or lake, while partial collapse due to permafrost thinning results in a bog (Johansson et al., 2006). Photographs, topographical survey and GHG data comparing Stordalen in the 1970's and 1980's to 2000's and 2010's show that for the particular area studied here the palsa has degraded both externally and internally (Fig S1, S2). Bogs (sphagnum or semi-wet) have expanded within the perimeter of the palsa-complex and around its southern edge, while fens (eriophorum, wet, or tall-graminoid) have encroached from the north, east, and west having converted the bog that once existed on the western and eastern edges of the palsa, along with increases in GHG emissions (Rydén et al., 1980; Malmer et al., 2005; Johansson et al., 2006; Bäckstrand et al., 2010). The majority of bog samples were taken from the subsided section within the palsa-complex, while the fen samples were taken from the western side of the complex, which was recorded as a bog 40 years ago. As permafrost continues to disappear from Stordalen over the coming decades, subsidence of the surface will likely increase, driving the creation of more transient bog-type communities and degradation into fens (Christensen, 2004; Parviainen and Luoto, 2007; Johansson and Åkerman, 2008; Fronzek et al., 2010; Bosiö et al., 2012; Jones et al., 2016). It is also predicted that this region could be free of permafrost as early as 2050 (Parviainen and Luoto, 2007; Fronzek et al., 2010). The "natural experiment" underway in the Mire presents a model ecosystem for investigating climate-driven changes in lowland permafrost regions with high cryosequestered-C (Masing et al., 2009).

As a model system, the Mire has been intensively studied over the last several decades for permafrost thaw impacts on plant communities, hydrology, and biogeochemistry – providing rich context for interpreting microbial communities. The

seasonally thawed peat layer (active layer) of Stordalen's palsas is drained, aerobic, ombrotrophic (rain-fed) and isolated from nutrient-rich groundwater. The palsa sites' low plant productivity and aerobic decomposition make them net emitters of appreciable CO_2 and no CH_4, with a net C balance (NCB) of - 30 mgC/m^2/day (negative value indicates net C emissions, positive indicates net uptake; Bäckstrand et al., 2010). In contrast, the bog sites (semi-wet in Johansson *et al* 2006) are physically lower and collect rainwater, leading to partial inundation, and are dominated by layered bryophytes (typically *Sphagnum* spp.). Although this results in less lignin (a recalcitrant C compound not produced by sphagnum), C degradation is still slow due to sphagnum's higher phenolic content (Freeman et al., 2004) and extremely poor C:N ratios of up to 70:1 (Hodgkins et al., 2014). Partially anoxic conditions permit microbial fermentation and CH_4 production (Nilsson and Bohlin, 1993; Hobbie et al., 2000). Mire bog sites have the lowest radiative forcing signature (NCB in CO_2 eq. of - 8 mgC/m^2/day; Bäckstrand et al., 2010), as fixation of C in the bog peat is high compared to emission of C gases. Finally, the fully-thawed fen sites (tall-graminoid in Johansson *et al* 2006) are the most subsided and are minerotrophic (groundwater-fed). Vegetation succession results in dominance of graminoids (sedges, rushes, reeds), with a subsequent shift in the litter preserved as peat. Some graminoids enhance gas transport between inundated soil and the atmosphere (Chanton et al., 1993) and due to high productivity, contribute appreciable fresh labile organic litter and exudates (Wagner and Liebner, 2009). High productivity results in the fens being the Mire's biggest gross C-sinks of the Mire, however their high CH_4 emissions result in a net warming potential 7 and 26 times greater than the palsa and bog respectively (NCB in CO_2 eq. of - 213 mgC/m^2/day, Bäckstrand et al., 2010; Christensen et al., 2012).

Here we explore the relationship between the biogeochemical differences among palsa, bog, and fen and the active layer microbial community, via a temporal (over a growing season) and spatial (across habitats, and with depth through the active

layer) community survey using SSU rRNA gene amplicon sequencing, pore-water chemistry, peat chemistry, stable C isotope analyses, and CH_4 flux. Previous work has demonstrated that permafrost thaw has an overall impact on Stordalen Mire's microbiota (Mondav & Woodcroft et al, 2014; Hodgkins et al., 2014; McCalley et al., 2014). Here, we deepen understanding of this impact by addressing the following descriptors with respect to climate-induced thaw and correlated environmental parameters: 1) dominant phyla, 2) beta diversity, 3) assemblage alpha diversity, 4) phylogenetic distance to identify drivers of assembly processes, 5) community network, and 6) C-cycling phylotype distribution.

Results and discussion

Dominant phyla of each thaw stage

Dominant phyla can inform on geochemical correlations and community functionality, reflecting overall habitat conditions. *Acidobacteria* and *Proteobacteria* were ubiquitous phyla across the Mire (Fig 1). Dominant palsa phyla also included *Actinobacteria* and Candidate bacterial phylum "WD272" (WPS-2), the abundances of which decreased across the thaw gradient (palsa>bog>fen). Surface bog samples had similar community composition to palsa samples being dominated by *Acidobacteria* and *Proteobacteria* suggesting that site classification, which was identified by vegetation, is not the only environmental correlate important to microbial community assembly in the Mire. Bog samples at or below the waterline (midpoint and deepest) retained similar proportions of *Acidobacteria* and *Actinobacteria* as palsa samples. *Proteobacteria* however, were relatively less abundant, likely due to lower C lability (Goberna et al., 2014; Hodgkins et al., 2014), and were replaced by *Euryarchaeota* in deeper anoxic samples. The shift in phylum ratios from palsa-like to fen-like supports the transitional nature of this thawing site. The most abundant phyla in the fen were *Euryarchaeota, Proteobacteria, Bacteroidetes*, and *Chloroflexi*

168 followed by *Acidobacteria. Woesearchaeota* (DHVEG-6) were only detected in fen
169 samples.

170 **<Fig 1, 110 mm wide>**

171 *Beta diversity and environmental correlates of site assemblages*

172 Microbial assemblages were significantly different (anosim r^2_{adj} = 0.90, p< 0.001) at
173 the sample OTU level between sites. Whole community analysis by nonmetric
174 multidimensional scaling (NMDS) (Fig 2a, stress = 0.082, r^2 = 0.99) clustered
175 samples by site. Samples separated along the primary NMDS axis according to
176 hydrological states with ombrotrophic (palsa and bog) samples clustered together left
177 of the origin and the minerotrophic fen samples to the far right. The secondary axis
178 separated samples according to depth from surface with the two ombrotrophic site
179 samples diverging from each other with depth. The palsa and surface bog
180 assemblages overlapped at both OTU (Fig 2) and phyla level (Fig 1). Sharing of
181 species across the palsa and surface bog (aerobic ombrotrophic) is likely due to
182 local dispersal and seen in other methanogenic soils (Kim and Liesack, 2015). Local
183 dispersal mechanisms include transport by burrowing lemmings, palsa dome runoff
184 washing microbes into lower altitudes, local aerial dispersal (Bowers et al., 2011).
185 Ubiquitous deposition across the mire via precipitation may also contribute (Christner
186 et al., 2008). These more ubiquitous microbes likely persist through environmental
187 filtering including oxygenation, acidity, ombrotrophy, and bryophyte presence (Brettar
188 et al., 2011; King et al., 2012).

189 C-fixing autotrophs were associated with all samples except the deepest bog and
190 fen. Bacterial methanotrophs, while distributed across the Mire, were not associated
191 with deep fen or deep bog samples, supporting their known preference for aerobic
192 and microaerobic habitats. Both autotrophs and methanotrophs were unique to
193 individual sites with only a few OTUs shared across the surface bog and palsa
194 samples. The majority of methanogenic phylotypes were clustered exclusively with

fen samples, though a secondary cluster of methanogens while more tightly associated to deep bog samples were detected across both bog and fen.

Relative increases in δ D_{H2O} and δ D_{CH4} were correlated with palsa sample assemblages (Fig 2a&b). This is indicative of methanotrophy as supported both by the detection of methanotrophic phylotypes but also by the negative CH_4 flux (uptake of CH_4 from atmosphere) recorded by the palsa auto-chambers. Increased peat C:N ratio, pore-water C:N, and porewater DOC were correlated with the bog assemblages supporting previous studies finding higher DOC in run-off from ombrotrophic regions of the Mire (Nilsson, 2006; Kokfelt et al., 2010) Pore-water N content decreased in relation to deeper bog samples. Increased pH, CH_4 flux from the auto-chambers, flux **δ** $^{13}C_{CH4}$ from the autochambers, pore-water **δ** $^{13}C_{CH4}$, and water table depth (WTD) were positively correlated with fen samples (Fig 2a). Pore-water CH_4 concentration, pore-water CO_2 concentration, CO_2 gas from peat samples, and pore-water total C increased with deeper (below watertable) bog and fen samples. Increased CH_4 in porewater and flux measurements were correlated to presence of detected methanogens (Fig 2b) supporting established linkage between detected abundance and metabolic activity of these microbes (Mondav et al., 2014).

<Fig 2, 110 mm wide>

Microbial assemblage alpha diversity

The number of unique OTUs per normalised (N=2000) sample ranged from 309 in the merged anoxic bog samples from august 2011 up to 1226 in the combined surface fen samples from june 2011 (Fig 3), with a cross-Mire mean OTU richness of 721 (s.d. 204 OTUs). The total richness was 9700 across the Mire for the 42 merged and normalised samples. The percentage of OTUs that could not be taxonomically classified either to or below order level was typical, at 40%, supporting that environmental microbes are still appreciably under-characterised. Total, archaeal, and bacterial assemblage alpha diversity as measured by richness (observed OTUs), Fisher alpha (Fisher et al., 1943), Shannon entropy (Shannon and Weaver,

1949), and Heip's evenness (Heip et al., 1974) varied between thaw stages, with there being a significant difference ($p < 0.05$) between sites as measured by Kruskal-Wallace test (K-W) (Fig 3). For total assemblage alpha diversity the bog had lowest (richness and fisher alpha), and was significantly lower than the palsa (shannons entropy and heips evenness) K-W post-hoc test for significance (K-Wmc, $p < 0.001$). The fen had highest archaeal alpha diversity (richness, fisher, and Shannon) while the palsa had most even archaeal assemblage (K-Wmc, $p < 0.001$). Apart from the exception of archaeal evenness the bog had lower or lowest alpha diversity of the three sites. Archaeal evenness in the bog site covers a wide range from assemblages with high evenness similar to that found in palsa samples but also includes assemblages that were more highly dominated than those found in the fen (Fig 3). Evenness is an important property of methane producing communities where higher evenness of fen assemblies, compared to bog samples, may constitute a feedback mechanism by which higher CH_4 production is enabled (Galand et al., 2003; Godin et al., 2012). Depth of sample was related to decreases in all alpha diversity metrics (total and bacterial, range: $-0.46 < \rho < -0.36$, $p < 0.01$). Bacterial ($r^2_{adj} = 0.92$, $p<0.001$) and total richness ($r^2_{adj} = 0.92$, $p<0.001$) decreased with depth in the bog while Archaeal richness increased ($r^2_{adj} = 0.69$, $p<0.001$) (Fig 3, Equations S1 a-c). Higher DOC correlated to lower richness (total $\rho = -0.76$, bacterial $\rho = -0.70$, and archaeal $\rho = -0.74$: $p<0.001$) (Fig S3). Bacterial richness was correlated to decreased porewater CO_2 ($\rho = -0.60$, $p<0.001$, Fig S3). Archaeal richness was positively correlated to distance below water-table ($\rho = 0.83$, $p<0.001$, Fig S3). The number of singletons observed in each site directly correlated with richness and varied between sites ($r^2_{adj} = 0.97$, $p<0.001$, Fig S4, Equations S1 d-g).

<Fig 3, 80 mm wide>

Site assembly dynamics

Links have been drawn between a community's diversity, functional and phylogenetic redundancy (robustness), and the community's ability to maintain function during

change (resistance), and to recover original state if the disturbance is removed (resilience) (Shade et al., 2012; Venail and Vives, 2013). While the degree to which phylogenetic and/or functional diversity influence resistance is not fully elucidated, recent studies support (Werner et al., 2011; Singh et al., 2014), these are important properties to consider with climate change and permafrost thaw, two interacting press disturbances at Stordalen (Shade et al., 2012; Hayes et al., 2014). A press disturbance is a change in the environment that persists for a long period of time, in comparison to a pulse disturbance which is a change that decreases suddenly after a short period of time. Phylogenetic robustness can be measured by various diversity relationships including phylogenetic distance between OTUs (PD); nearest taxon index (NTI), which examines phylogenetic clustering of closely related phylotypes; and mean relatedness index (NRI) which examines variance of phylotype distance within an assemblage. Further, these indices can indicate the relative degree to which stochastic or deterministic processes contribute to community assembly (Wang et al., 2013). The Mire as a whole and each site individually had positive correlation (r^2_{adj} = 0.73 to 0.94, $p<0.001$) between overall phylogenetic diversity (PD) and richness (Eqs S2a-d, Fig S5). Because PD and richness were auto-correlated, subsequent analyses examined PD/OTU so as to examine only the difference due to diversity and not an artefact of abundance counts. Fen PD/OTU was significantly ($p<0.001$) higher than both bog and palsa assemblages (Fig 4). Measuring assemblage net relatedness (NRI, equivalent to -sesMPD) by OTU phylogenetic distance from sample mean as generated by the null model examines clustering over a whole tree. Greater emphasis is placed on changes towards the tree root compared to other measures such as NTI, which examines diversity at the tips of the phylogenetic tree. Negative values of NRI indicate expansion of the tree via increased branching at higher-level tree nodes i.e. even-dispersal, while positive values indicate filling in of internal phylogenetic tree nodes i.e. clustering. Palsa assemblages had uniformly high NRI, ($0.1 < NRI < 0.4$,

279 Fig 4) indicative of phylogenetic clustering. A deterministic factor associated with
280 clustering specific to the palsa (and surface bog) is dry-ombrotrophy which increases
281 habitat isolation in heterogeneous soil environments (Kraft et al., 2007; Jones et al.,
282 2009; Stegen et al., 2013; Quiroga et al., 2015). Fen assemblage NRIs were
283 significantly lower than the other sites (KW, $p<0.001$, Fig 4) and were neutral to
284 negative. Bog assemblage NRIs varied ($0 < NRI < 0.4$) from neutral in deeper
285 samples to higher than some Palsa in surface samples (Fig 4, Fig S5, Eq S4). The
286 lower NRI in the fen indicates assemblages have broader representation across the
287 bacterial and archaeal domains with less clustering than predicted by the null model
288 i.e. phylogenetic even dispersal. Even dispersal can indicate an assemblage less
289 affected by deterministic processes such as habitat filtering or isolation (Webb et al.,
290 2002; Horner-Devine and Bohannan, 2006), while being more affected by stochastic
291 processes such as dispersal and drift or controversially, by competition (Mayfield and
292 Levine, 2010). All assemblage NTI values were above zero, i.e. more clustered than
293 predicted with the null model, a result seen in early stage successional forests and
294 freshwater mesocosms, (Horner-Devine and Bohannan, 2006; Whitfeld et al., 2012).
295 The bog and fen had greater phylogenetic tip clustering than the palsa (KW $p < 0.05$,
296 Fig 4) and was, in the bog, related to depth (Eq S3). Greater tip-clustering as seen in
297 the bog and fen indicates greater genomic diversification within 'species'-
298 populations. This could be achieved through horizontal gene transfer (HGT) or
299 endogenous mutation enabling more closely related organisms to coexist (Goberna
300 et al., 2014), though there is not yet data to address effective population sizes, or the
301 relative frequencies of HGT and endogenous genome mutation in these habitats.
302 The ratio of NRI to NTI indicates the level (tree:tip) at which phylogenetic diversity is
303 affected by assembly processes. Fen assemblages had significantly greater
304 clustering at the whole tree level than tree tip when compared to the other sites
305 (NRI/NTI, Fig 4, $p<0.01$). Conversely, the palsa assemblages displayed greater
306 clustering towards the tree's tips. The bog NRI/NTI was in-between the palsa and the

fen. This shift in where the assemblage diversity lies supports clustering through local species divergence being a property of the ombrotrophic mire sites while even-dispersal is more prevalent in the minerotrophic fen. The clustering shift from tip to whole tree diversity is also seen at a smaller scale within the bog site (Fig S5, Eq S5) where surface samples have higher tip clustering and deeper samples have more evenly distributed diversity. That the mid depth bog samples were taken at the waterline supports that a main factor regulating this shift is inundation by water. Phylogenetic diversity of Mire assemblages as measured through PD, NRI, and NTI showed the bog grouping alternately with the palsa or the fen supporting that the bog may be an intermediate site undergoing transition from a palsa-like assemblage to fen-like assemblage due to a shift from ombrotrophy to minerotrophy. These four phylogenetic distance analyses support that each site has a unique overall phylogenetic diversity profile, thus giving support to there being differences in assembly and evolution of the microbial community across sites and therefore thaw stages (Stegen et al., 2012).

Examining correlations between environmental parameters and phylogenetic diversity can potentially inform on the relative contribution, directly or indirectly, of environmental to assembly processes. Phylogenetic clustering related to environmental filtering is predicted to be evident in environments with poor nutrient availability or parameters considered to increase selection such as high acidity. Phylogenetic evenness, conversely, is expected to be evident in environments with high resource availability where competition becomes more dominant in assembly processes. Increasing soil pH, ratio of methanogens to methylotrophs, CH_4 flux, and distance below watertable were significantly correlated to increasing PD/OTU and decreasing NRI and NRI/NTI ($\rho \geq \pm 0.60$, $p<0.001$, Table S2, Fig S6) i.e. associated with phylogenetic even dispersal. Greater depletion of $^{13}C_{CH4}$, higher porewater DOC, and higher porewater C:N ratios were correlated to decreasing PD/OTU and increasing NRI, and NRI/NTI i.e. phylogenetic clustering ($\rho \geq \pm 0.60$, $p<0.001$, Table

S2). Only bog and fen porewater DOC and C:N were analysed as there was insufficient moisture in the palsa samples. Conditions associated with environmental filtering (acidity) and isolation (ombrotrophy) may here be linked to phylogenetic clustering (Kraft et al., 2007). Stochastic mechanisms specific to the fen include inflow of runoff from the raised palsa and bog, minerotrophy, and local water mixing which reduces isolation (Putkinen et al., 2012). Conditions associated with phylogenetic even-dispersal may therefore be linked to warming potential (increased CH_4 flux) and increases in acetotrophic methanogens (less depletion of ^{13}C in CH_4 emissions) in methanogenic soils. Clustering is an emerging characteristic of soil communities (Lozupone and Knight, 2007; Auguet et al., 2010) that is currently connected to habitat filtering (Kraft et al., 2007; Shade and Handelsman, 2012) though some recent evidence also supports a role for biotic filtering (Goberna et al., 2014). The correlations between higher phylogenetic diversity, including even-dispersal, and CH_4 flux corroborate findings from reactors and environmental systems (Werner et al., 2011; Yavitt et al., 2011) that the structure of microbial communities may be significant to global CH_4 budgets.

<Fig 4, 80 mm wide>

Network topology and community interactions

Microbial networks can be described mathematically by topological indices. Common indices include degree, modularity, betweenness, and closeness. Degree describes the level of connectedness between phylotypes by counting the number of phylotypes that co-occur. Modularity identifies if sub-networks of co-occurrence exist within a larger community network and is thought to be an indicator of resilience. Betweenness Centrality provides information on how critical a phylotype is to the connectedness of a network. Closeness Centrality describes how closely a phylotype is connected to all others in the same module. Redundancy (e.g similar metabolic strategies) is also a useful descriptor of co-existing organisms. Degree, closeness and redundancy in microbial networks provide information on the community's

363 robustness and, potentially, ability to resist change. OTU Table B_{2000} had 9 700
364 unique phylotypes, 93% sparsity, average inverse Simpsons (n_{eff}) of 122 per sample
365 which was too sparse to obtain meaningful network information from. Restricting the
366 dataset to OTUs that were present in at least 15 samples (one third of total) left 257
367 unique OTUs, a table with 49% sparsity, and an average n_{eff} of 26, statistics that
368 provide assurance that network interactions could be correctly identified while
369 minimising type I errors (Friedman and Alm, 2012; Berry and Widder, 2014; Weiss et
370 al., 2016). Retaining only OTU pairs that were significantly correlated in at least two
371 of the network analyses from MENA, fastLSA, CoNet (Pearsons, Spearman, Bray,
372 KBL), and SparCC reduced the dataset to 123 OTUs with 265 significant pairwíse
373 correlations (Table S3). The network had low degree (average 4.3 per node), a
374 maximum path of 14, and low checkerboard (C-score= 0.387). The C-score was
375 compared to the null model and found to be different (null model C-score = 0.338)
376 with a 97.5% CI and $p<0.001$ supporting non-random OTU co-occurrence patterns
377 and the presence of a microbial network. However the work by Berry and Widder
378 (2014) examining the effect of filtering on sensitivity indicates that type II errors may
379 be as high as 0.5 based on 16-20% of the network potentially being habitat
380 specialists (Table S4). Analysis and visualisation of this network (Fig 5) revealed a
381 community consisting of 8 modules.
382 The detection of phylotypes in different environments, and their network topological
383 description, enables exploration of community metabolic roles of microbial lineages
384 (Foster et al., 2008). Highly connected phylotypes sometimes called hubs or
385 keystones (high degree, high closeness, low betweenness) are predicted to perform
386 key metabolic steps within microbial communities. In the identified network at
387 Stordalen only hubs with high degree, high closeness but with high betweenness
388 were identified (Fig 5, Table S3 & S4). Due to their high betweenness and close
389 phylogenetic relatedness to adjacent OTUs these hubs exhibit qualities associated
390 with redundancy or 'niche overlap' and therefore may have little effect if removed i.e.

391 they are unlikely keystone species. Keystone species, while sometimes described
392 statistically as hubs (Faust and Raes, 2012; Berry and Widder, 2014), are
393 ecologically those that would cause (disproportionate) disruption to a network if lost.
394 In the larger modules of the network, there were a few phylotypes (putative
395 keystones marked on Fig 5, Table S3, S4) that if removed would fragment the
396 network and/or were the only phylotypes identified as associated with a critical
397 metabolic process. The loss of any of the identified keystone phylotypes from any of
398 the three sites, past or future, could affect significant changes in C, N, S, or Fe
399 cycles at Stordalen. Identification of keystone species is problematic if there is a high
400 degree of type II errors or, as is expected with environmental phylogenetic-amplicon
401 surveys, there is limited information available on their phenotypes. Statistically, the
402 predicted keystones in this network cover the full range of betweenness and
403 closeness scores but none had high degree, supporting that high degree is a poor
404 predictor of 'keystoneness' in soil microbial communities.
405 Module 'A' consisted of 25 phylotypes (19 Acidobacteria, 4 Actinobacteria, 2
406 Euryarchaeota) that were dominant in the bog (Fig 5, Table S4). Two of the
407 *Acidobacteriaceae* (subgroup I Acidobacteria) phylotypes were identified as hubs.
408 The potential keystones (based on topology) were another *Acidobacteraceae* and
409 the less abundant of the two *Ca.* Methanoflorens (RCII) phylotypes. *Ca*.
410 Methanoflorens is a hydrogeno/formatotrophic methanogen of the *Methanocellales*
411 order that prefer low H^2 concentration, and are oxygen and acid tolerant (Sakai et al.,
412 2010; Lü and Lu, 2012; Mondav et al., 2014; Lyu and Lu, 2015). One of the three
413 *Acidobacteria* identified at genus level was a phylotype of *Ca*. Solibacter. Solibacter
414 are capable of degrading complex-C molecules such as cellulose, hemicellulose,
415 pectin, chitin, and starch (Ward et al., 2009; Pankratov et al., 2012), a useful
416 phenotype in the sphagnum-peat of the bog. Another was an *Acidobacterium* that
417 may be able to reduce ferric iron (Coupland and Johnson, 2008). The last of the
418 genus level identified was an *Acidcapsa* which likely preferentially utilise bi-products

of sphagnum degradation such as xylose or cellobiose, but if necessary could directly degrade starch and pectin (Kulichevskaya et al., 2012; Matsuo et al., 2016). The four *Acidimicrobiales* identified might contribute to Fe-cycling and likely capable of degrading complex polymers (Kämpfer, 2010; Stackebrandt, 2014). The remainder of module A (unknown *Acidobacteraceae*) are likely chemoheterotrophs that either degrade sphagnum derived polymers or their hydrolysed bi-products (Campbell, 2014). Eighty percent of module A phylotypes had significant positive correlations ($\rho \geq \pm 0.60$, $p_{ad} < 0.001$, Table S5) with porewater N, DOC concentration.

Module B ^{total} was the most phylogenetically and phenotypically mixed module, it was further divided into two sub-modules: B and B'. Thirty-four of module B phylotypes were only detected in the fen, eight in both bog and fen samples, and three in both fen and palsa samples. Module B hubs included both of the *Bacteroidetes* phylotypes, a *Woesearchaeota* (DHVEG-6) and a *Methanosaeta*, and a *Methanoregula* and a *Bathyarchaeota* (Msc. Crenarcheaota Grp) (Fig 5, Table S4). The *Bacteroidetes* phylotypes are likely anaerobic, organotrophs with a preference for sugar molecules (Krieg et al., 2010). *Methanosaeta* are obligate acetotrophic methanogens and their higher substrate (acetate) affinity may be one mechanism enabling them to compete in the fen (Westermann et al., 1989; Ferry, 2010; Liu et al., 2010) as would the higher pH and reduction in inhibitory phenolics compared to conditions in the bog. A *Methanoregula* phylotype was also identified as a hub, the only potentially hydrogenotrophic (&/or formatotrophic) methanogen in module B. Its requirement for and greater tolerance of acetate, might assist *Methanosaeta* by using up some of the available acetate (Smith and Ingram-Smith, 2007; Bräuer et al., 2011; Oren, 2014b). No phenotypic data is yet available for *Woesearchaeota.* and the *Bathyarchaeota* so far described were either methanogenic, methanotrophic, or organoheterotrophic (Butterfield et al., 2016; Lazar et al., 2016). So while no predictions can be made as to whether these phylotypes are e.g. methanogens, it is evident that they are important methanogenic-community members. One of the

447 methanogenic phylotypes connected to the Woesearchaeota and Bathyarchaeota
448 was a methylotrophic-methanogen of the *Methanomassiliicoccus* genus (Borrel et
449 al., 2013). Module B and B' were connected by the co-occurrence of one of these
450 *Bathyarchaeota* and a *Methanobacterium* respectively, both possible keystones. The
451 other putative keystones were an actinobacterial phylotype of the *Gaiellales* order of
452 unknown but likely heterotrophic metabolism, and the chemolithoautotrophic
453 *Nitrospiraceae* (Daims, 2014). It is probable that the *Nitrospiraceae* phylotype, which
454 was not detected in the bog, contributes to the module by C-fixation (Daims, 2014).
455 Two other module B phylotypes not in the bog were a chemoorganotrophic
456 (putative complex-C degrader) *Myxococcales* genus *Haliangium* (Kim and
457 Liesack, 2015), and an uncultured *Chloroflexi* KD4-96. The thirteen OTUs of
458 module B' were either not detected or detected at very low abundance in the palsa
459 (Fig 5, Table S4). All B' phylotypes were methanogens from either the
460 hydrogeno/formatotrophic *Methanobacterium* genus or the metabolically flexible
461 *Methanosarcina* genus (Oren, 2014a, 2014c). Module B', and to a lesser extent B,
462 displays the functional redundancy and phylogenetic clustering characteristic of soil
463 communities and in particular methanogenic soils (Embree et al., 2014). Module B
464 phylotypes (87 %) were strongly correlated ($\rho \geq \pm 0.60$, $p_{adj}<0.001$, Table S5) to
465 phylogenetic even dispersal (NRI), pH, CH4 flux, and decreasing porewater N.
466 Module C consisted mainly of *Xanthomonadales* an order of obligate aerobic
467 *Gammaproteobacteria* capable of degrading complex organic molecules and
468 participating in methyl / H syntrophic partnerships with methylotrophs (Kim and
469 Liesack, 2015). The co-presence of the keystone methylotrophic proteobacterial
470 *Methylotenera* (Doronina et al., 2014) phylotype supports the possibility that such
471 partnerships occur at Stordalen and are common in the aerobic partition of
472 methanogenic soils. A second keystone phylotype was the C-fixing verrucomicrobial
473 methanotroph *Methylacidiphilum* (Hedlund, 2010; Sharp et al., 2013). The final
474 keystone was the putative ferric iron reducing, H_2/CO_2 producing *Acidocella*. which

may also have a syntrophic partner within module C (Coupland and Johnson, 2008; Johnson and Hallberg, 2008). Most phylotypes (12 of 16) were correlated to increased clustering (NRI) and acidity (Table S5).

Module D consisted of 14 OTUs, nine *Acidobacteria,* four *Gammaproteobacteria* (*Xanthomonadales*), and one *Verrucomicrobia* all of whom were dominant in the palsa. Three keystones were identified, a subdivision 2 Acidobacteria, a Bryobacter (subdivision 3 Acidobacteria), and a putatively ferric iron reducing Acidobacterium (subdivision 1 Acidobacteria) phylotype. Bryobacter are chemoheterotrophs with a preference for sugars (Dedysh et al., 2016). This module appears to have members that together degrade complex-C molecules, polysaccharides and simple sugars (Hedlund, 2010; Dedysh et al., 2016; Yang et al., 2016). Twelve of the phylotypes had significant correlation ($\rho \geq \pm 0.60$, $p_{adj}<0.001$, Table S5) with distance above frozen ground/watertable. Module E had five *Syntrophobacterales* phylotypes, putative producers of substrates for methanogenesis (acetate, H, and formate) and capable of N fixation (Embree et al., 2014; Lin et al., 2014), with four from the *Smithella* genus and one from *Syntrophus*. None of these five were detected in palsa samples. The final OTU of the module was detected across the mire and identified as belonging to the *Verrucomicrobia* OPB35 soil group which is thought to degrade polysaccharides (Hedlund, 2010; Yang et al., 2016). All of module E phylotypes were significantly correlated with increasing CH_4 flux and decreasing NRI ($\rho \geq \pm 0.60$, $p_{adj}<0.001$, Table S5).

Overall, the clustering of closely related phylotypes in modules is consistent with the phylogenetic diversity results. The network associations of methanogen phylotypes were complex and modular, with most falling into sub-network B' (present in bog and fen and low abundance in palsa), followed by B (fen only, except for the more cosmopolitan *Methanomasilliicoccus* phylotype). The two outlying *Ca.* Methanoflorens methanogens in module A (fen and bog) were associated with Acidobacteria and Actinobacteria which are typical of peat environments and The

503 presence of permafrost fits the known distribution of this genus (Mondav et al., 2014)
504 and its predicted phenotype. The putative C-fixing autotrophs were scattered through
505 the network and only moderately connected, supporting their phylogenetically-based
506 assignments to a primary trophic role.

507 **<Fig 5, 169 mm wide>**

508 *Known C-cycling phylotypes*

509 Distinct shifts in relative abundances of putative methanogens, and methylotrophs
510 were evident across the Mire. Relative abundance of methanogens increased across
511 the thaw gradient (palsa<bog<fen, Table S6) (K-Wmc, p <0.001). Methanogens were
512 strongly associated with the deepest bog and fen samples (Table S6, Fig S7). All but
513 one of the obligate acetotrophic methanogens (*Methanosaeta*) were detected
514 exclusively in the fen (Fig S7), the other one was found in a single palsa sample.
515 Apart from the anomalous *Methanosaeta* detected in the palsa, this is consistent with
516 reported acetotrophic sensitivity to low pH due to reduction of the ΔG (Gibbs free
517 energy) of the acetotrophic methanogenesis pathway (Kotsyurbenko et al., 2007).
518 The possibility of a divergent metabolism may explain the presence of the
519 *Methanosaeta* in the palsa. Other methanogenic phylotypes detected in apparently
520 aerobic samples (above the water line) may have been enabled by micro-anaerobic-
521 habitats, oxidative resistance as seen in some *Methanocellales* (Angel et al., 2011),
522 or association with an anaerobic host gut (Paul et al., 2012). Putative
523 methano/methylotrophic phylotypes were distributed across all samples (Fig S7) and
524 were highest in the bog samples (K-Wmc, p <0.01,Table S6) likely accounting for the
525 lower CH_4 flux despite the abundance of methanogens. Some methylotrophs were
526 detected below the waterline in bog and fen samples (Fig S7) and likely exist in
527 micro-aerobic spaces enabled by plant root gas transport (Colmer, 2003). The
528 relative ratio of methanogen to methanotroph phylotypes differed significantly
529 between sites (K-Wmc, p <0.01), increasing across the thaw gradient
530 (palsa<bog<fen, Table S6). Due to the polyphyletic distribution of autotrophic and

methanotrophic metabolisms the assignment of function requires identification to family or genera level, while most methanogens can be identified at class or order level. It is therefore likely that abundances and richness of autotrophic and methanotrophic microbes described here are underestimated more than methanogens. The shifting C-cycling phylotype patterns described here, especially the methanogen to methanotroph ratio provide detail of biogenic methane production and consumption that support reported site C-budgets (Bäckstrand et al., 2010), CH_4 emissions and CH_4 isotope ratios (McCalley et al., 2014) from Stordalen.

The presence of permafrost maintains the ombrotrophic, acidic environment (Natali et al., 2011; Tveit et al., 2013) which correlated with a diverse, rich, phylogenetically-clustered, and autotroph-abundant palsa community. The bog sites (thawing permafrost) had significantly lower richness, diversity, evenness and estimated population size than the palsa, the fen, and also other peat bog sites (Lin et al., 2012; Serkebaeva et al., 2013; Tveit et al., 2013). Collectively, this suggests a structural response to ecosystem disturbance (Degens et al., 2001) caused by site inundation as a consequence of subsidence caused by permafrost thaw (Rydén et al., 1980; Johansson and Åkerman, 2008). Correlations between diversity estimates (alpha, beta, and phylogenetic) and distance of sample above or below the water table support that site inundation (and therefore thaw) is a mechanistic driver of community structure and function and that deterministic processes were the main drivers of community composition and assembly in this and other bogs (Quiroga et al., 2015). Complete loss of permafrost in the fen was correlated to assemblages with highest richness, alpha diversity, beta diversity, and phylogenetic even-dispersion.

As the permafrost thaws, causing subsidence, Palsas and transitory bogs at Stordalen mire are expected to give way to fens. At Stordalen the transition from bog to fen is accompanied by community diversification and proliferation of methanogens and a decrease in the relative ratio of methanotrophs. It appears at Stordalen, as

found elsewhere under similar conditions (Liebner et al., 2015), that at the point of inundation a regime shift is initiated and that beyond this point, the community does not recover but instead shifts towards a new stable state as found in the fen. The fen assemblage has qualities indicative of greater stability (high redundancy, evenness, richness, and diversity) coincident with an altered C-budget of dramatically higher warming potential. The combination of changes predicted by climate models, the trajectory suggested in biogeochemical and vegetation surveys of the Mire, and the details of the microbial community C-cycling shifts detailed here suggest that the mires along the Torneträsk valley will increasingly add to radiative climate forcing via increased CH_4 flux over the coming decades as more land is converted to fen. Longer-term outcomes of climate change in this region are projected to eventually include some drying (e.g. terrestrialisation, the conversion of wetlands to drier areas (Payette et al., 2004)) and expansion of the dwarf forests (Rundqvist et al., 2011). If these fundamental habitat shifts occur, they are extremely likely to drive further changes in the microbial communities and C budgets of the region.

Experimental Procedures

Field site and sampling

Samples were taken from the active layer of an individual palsa thaw sequence in Stordalen Mire, subarctic Sweden (68.35N, 19.04E), with three stages of permafrost degradation evidenced by topographical and vegetative characteristics (intact, thawing, and thawed; Fig S1). The intact permafrost was represented by a raised section of the palsa (palsa site, Fig S2); the thawing transition site was an elevationally depressed region within the palsa (bog site); and the thawed permafrost was a thermokarst feature with no detectable permafrost and thus no apparent seasonal active layer (fen site) (Rydén et al., 1980; Malmer et al., 2005). The palsa site was an ombrotrophic, drained, raised peat (altitude 351 m.a.s.l (Jackowicz-Korczyński et al., 2010)) with tundra vegetation including *Betula nana* and *Empetrum*

587 *hermaphroditum*, interspersed with *Eriophorum vaginatum, Rubus chamaemorus*,
588 lichens, and mosses. The bog site was a wet ombrotrophic depression sunken ~1 m
589 below the palsa. Vegetation was predominately *Sphagnum spp*. with *E. vaginatum*.
590 Water table varied seasonally from 5 cm above to 30 cm below the vegetation
591 surface and was perched above the local groundwater. The average pH of the
592 ombrotrophic sites was 4.2 +/- 0.3 sd. The fen site was a minerotrophic, waterlogged
593 fen ~2 m below the palsa, vegetation was dominated by *Eriophorum angustifolium*
594 with some *Sphagnum spp*. and *Equisetum spp*., and open water was present. The
595 water table was always within 5 cm of the peat surface, sometimes being above it,
596 and average pH of 5.7 +/- 0.1 sd.
597 Soil cores were taken in August/September 2010 and June, July, August, and
598 October 2011 (Table S1, Table S7). On each of the five sampling dates, between two
599 and four cores were taken from each of the three sites (Fig S1). In 2010 four cores
600 were taken from palsa and bog sites, in October 2011 two cores were taken from the
601 fen site, and all remaining sampling dates and locations had three cores sampled.
602 Samples cut from cores taken from the same site, at either the same depth in cm or
603 the same ecologically significant depth (e.g. depth relative to water table) were
604 designated technical replicates. Samples taken at different depths were analysed as
605 treatments (Samples taken at different depths were selected based on ecologically
606 pre-determined indicators such as at the water table for the bog, Fig S2). Porewater,
607 peat, flux and isotope measurements taken simultaneously to the microbial samples
608 were described in Mondav et al. (2014), Hodgkins et al. (2014) and McCalley et al
609 (2014) but are detailed again in the Supplementary Methods.
610 *SSU rRNA gene amplicon sequencing and analysis*
611 Microbial community was surveyed by small subunit (SSU) rRNA gene amplicon
612 sequencing (Mondav et al., 2014). Briefly, DNA was amplified with tagged primers for
613 V6-V8 region of the SSU rRNA gene with the 926F (AAACTYAAAKGAATTGRCGG)
614 and 1392wR (ACGGGCGGTGWGTRC) primers, in duplicate reactions, pooled, and

615 sequenced with the 454 Ti GS (LifeSciences, Carlsbad). Sequences are available
616 from SRA under accession SRA096214 (McCalley et al., 2014; Mondav et al., 2014),
617 SRR numbers and primer details are listed in detail in Table S1. Sequences were
618 cleaned (pre-processed) with MacQIIME v1.9.1 then analysed at an operational
619 taxonomic unit (OTU) of 97% identity. A detailed description of pre-processing
620 methods can be found in the Supplementary Methods. Cleaned sequences were
621 assigned taxonomy using the open picking method and the SILVA database and a
622 phylogenetic tree made with Fasttree2 and manually rooted between the archaeal
623 and bacterial domains (Caporaso, Bittinger, et al., 2010; Caporaso, Kuczynski, et al.,
624 2010; Edgar, 2010; Price et al., 2010; Huson and Scornavacca, 2012; McDonald et
625 al., 2012; Quast et al., 2013). Phylotype lineage obtained by assignment of reads to
626 taxon identity was utilised to assign putative C-metabolism. Phylotypes that were
627 assigned to lineages with known methanogen, methanotroph/methylotroph, and C-
628 fixing members were manually checked before C-metabolism was assigned.

629 *Microbial assemblages*

630 Phylum level analysis was obtained by collapsing the normalised OTU table in
631 Qiime, and phyla detected in more than one sample and also present at over 1% in
632 at least one sample were graphed in MS Excel. To investigate dissimilarity of sample
633 and site assemblages a non-parametric ordination (NMDS) was done in R v3.3.1 (R-
634 Core-team, 2011) using the RStudio v0.99.903 (RStudio, 2012) IDE with the vegan
635 package v2.4-1 (Oksanen et al., 2013) and plotted using gplots v3.0.1 and with
636 scales v0.2.3 (Warnes et al., 2011). Environmental variables and parameters were
637 fitted to the NMDS and factors with significant ($p < 0.05$) correlation plotted. Alpha
638 diversity metrics were generated in Qiime (richness, singletons, Shannon diversity,
639 Fisher alpha, Heip's evenness, Simpson's dominance and Chao1 estimates) and
640 analysed in R using the non-parametric Kruskal-Wallis (K-W) followed by post-hoc
641 testing with Kruskal-Wallis multiple comparison (K-Wmc) testing using R package
642 pgirmess v1.6.4 (Giraudoux, 2012). Correlation analyses were done using non-

parametric Spearman and linear regression and differences between sites were checked for significance with the largest p value obtained reported. Images were processed for publication in Inkscape 0.91. Analysis of the phylogenetic diversity and distance (PD, NRI, NTI) were calculated using the distance tree output from QIIME, and correlation and equations calculated in R with picante v1.6-0 (Gotelli, 2000; Faith, 2006; Kembel et al., 2010). OTUs present in less than 15 samples were removed and the resultant OTU table analysed for pairwise interactions in MENA (Deng et al., 2012), fastLSA (Durno et al., 2013), CoNet v1.1.1 (Faust et al., 2012) and SparCC (Friedman and Alm, 2012). All networks were loaded into R and OTU pairs that were identified as present in at least two of the four networks were retained and the network analysed in CytoScape v3.4.0. See Supplementary Methods for detailed description of all methods.

Supplementary Information is available as a separate download and includes Supplementary Methods, Figs S1-S7, Equations S1-S5, and Tables S1-S7.

Acknowledgements

Many thanks to Andrew C Barnes, Brian Lanoil, and James Prosser for critical comments on a previous version of the manuscript. Sincere thanks to the two anonymous reviewers who helped me greatly improve this manuscript. RM was supported by an Australian Postgraduate Award Scholarship and a Swedish Vetenskapsrådet grant. JPC, PMC, SF, SH, CKM, SRS, and VIR were supported by the US Department of Energy, Office of Biological and Environmental Research under the Genomic Science program (Award DE-SC0004632).

Author contributions

669 JPC, PMC, SF, SRS, VIR designed the project. RM designed and performed all
670 bioinformatics analyses and visualizations. RM wrote the paper in consultation with
671 all authors.
672
673 **References**

674 Alewell, C., Giesler, R., Klaminder, J., Leifeld, J., and Rollog, M. (2011) Stable carbon
675 isotopes as indicators for environmental change in palsa peats. *Biogeosciences*
676 **8**: 1769–1778.
677 Angel, R., Matthies, D., and Conrad, R. (2011) Activation of methanogenesis in arid
678 biological soil crusts despite the presence of oxygen. *PLoS One* **6**: e20453.
679 Bäckstrand, K., Crill, P.M., Jackowicz-Korczyñski, M., Mastepanov, M., Christensen,
680 T.R., and Bastviken, D. (2010) Annual carbon gas budget for a subarctic
681 peatland, Northern Sweden. *Biogeosciences* **7**: 95–108.
682 Bäckstrand, K., Crill, P.M., Mastepanov, M., Christensen, T.R., and Bastviken, D.
683 (2008) Total hydrocarbon flux dynamics at a subarctic mire in northern Sweden.
684 *J. Geophys. Res.* **113**: G03026.
685 Berry, D. and Widder, S. (2014) Deciphering microbial interactions and detecting
686 keystone species with co-occurrence networks. *Front. Microbiol.* **5**: 1–14.
687 Bhiry, N. and Robert, É.C. (2006) Reconstruction of changes in vegetation and
688 trophic conditions of a palsa in a permafrost peatland. *Ecoscience* **13**: 56–65.
689 Borrel, G., O'Toole, P.W., Harris, H.M.B., Peyret, P., Brugère, J.-F., and Gribaldo, S.
690 (2013) Phylogenomic data support a seventh order of Methylotrophic
691 methanogens and provide insights into the evolution of Methanogenesis.
692 *Genome Biol. Evol.* **5**: 1769–80.
693 Bosiö, J., Johansson, M., Callaghan, T. V., Johansen, B., and Christensen, T.R.
694 (2012) Future vegetation changes in thawing subarctic mires and implications
695 for greenhouse gas exchange—a regional assessment. *Clim. Change* **115**: 379–
696 398.

Bowers, R.M., McLetchie, S., Knight, R., and Fierer, N. (2011) Spatial variability in airborne bacterial communities across land-use types and their relationship to the bacterial communities of potential source environments. *ISME J.* **5**: 601–612.

Bräuer, S.L., Cadillo-Quiroz, H., Ward, R.J., Yavitt, J.B., and Zinder, S.H. (2011) Methanoregula boonei gen. nov., sp. nov., an acidiphilic methanogen isolated from an acidic peat bog. *Int. J. Syst. Evol. Microbiol.* **61**: 45–52.

Brettar, I., Christen, R., and Höfle, M.G. (2011) Analysis of bacterial core communities in the central Baltic by comparative RNA-DNA-based fingerprinting provides links to structure-function relationships. *ISME J.* 1–18.

Butterfield, C.N., Li, Z., Andeer, P.F., Spaulding, S., Thomas, B.C., Singh, A., et al. (2016) Proteogenomic analyses indicate bacterial methylotrophy and archaeal heterotrophy are prevalent below the grass root zone. *PeerJ* **4**: e2687.

Campbell, B.J. (2014) The family acidobacteriaceae. In, *The Prokaryotes: Other Major Lineages of Bacteria and The Archaea*. Springer Berlin Heidelberg, Berlin, Heidelberg, pp. 405–415.

Caporaso, J.G., Bittinger, K., Bushman, F.D., Desantis, T.Z., Andersen, G.L., and Knight, R. (2010) PyNAST: A flexible tool for aligning sequences to a template alignment. *Bioinformatics* **26**: 266–267.

Caporaso, J.G., Kuczynski, J., Stombaugh, J., Bittinger, K., Bushman, F.D., Costello, E.K., et al. (2010) QIIME allows analysis of high- throughput community sequencing data. *Nat. Methods* **7**: 335–336.

Chanton, J.P., Whiting, G.J., Happell, J.D., and Gerard, G. (1993) Contrasting rates and diurnal patterns of methane emission from emergent aquatic macrophytes. *Aquat. Bot.* **46**: 111–128.

Christensen, T.R. (2004) Thawing sub-arctic permafrost: Effects on vegetation and methane emissions. *Geophys. Res. Lett.* **31**:.

Christensen, T.R., Jackowicz-Korczyński, M., Aurela, M., Crill, P.M., Heliasz, M.,

725 Mastepanov, M., and Friborg, T. (2012) Monitoring the Multi-Year Carbon
726 Balance of a Subarctic Palsa Mire with Micrometeorological Techniques. *Ambio*
727 **41**: 207–217.
728 Christensen, T.R., Johansson, T., Åkerman, J.H., Mastepanov, M., Malmer, N.,
729 Friborg, T., et al. (2004) Thawing sub-arctic permafrost: Effects on vegetation
730 and methane emissions. *Geophys. Res. Lett.* **31**: 1–4.
731 Christner, B.C., Morris, C.E., Foreman, C.M., Cai, R., and Sands, D.C. (2008)
732 Ubiquity of biological ice nucleators in snowfall. *Science* **319**: 1214.
733 Colmer, T.D. (2003) Long-distance transport of gases in plants: a perspective on
734 internal aeration and radial oxygen loss from roots. *Plant, Cell Environ.* **26**: 17–
735 36.
736 Coupland, K. and Johnson, D.B. (2008) Evidence that the potential for dissimilatory
737 ferric iron reduction is widespread among acidophilic heterotrophic bacteria.
738 *FEMS Microbiol. Lett.* **279**: 30–35.
739 Daims, H. (2014) The family nitrospiraceae. In, *The Prokaryotes: Other Major*
740 *Lineages of Bacteria and The Archaea*. Springer Berlin Heidelberg, Berlin,
741 Heidelberg, pp. 733–749.
742 Dedysh, S.N., Kulichevskaya, I.S., Huber, K.J., and Overmann, J. (2016) Defining
743 the taxonomic status of described subdivision 3 Acidobacteria: the proposal of
744 Bryobacteraceae fam. nov. *Int. J. Syst. Evol. Microbiol.*
745 Degens, B.P., Schipper, L.A., Sparling, G.P., and Duncan, L.C. (2001) Is the microbial
746 community in a soil with reduced catabolic diversity less resistant to stress or
747 disturbance? *Soil Biol. Biochem.* **33**: 1143–1153.
748 Deng, Y., Jiang, Y.H., Yang, Y., He, Z., Luo, F., and Zhou, J. (2012) Molecular
749 ecological network analyses. *BMC Bioinformatics* **13**: 113.
750 Doronina, N., Kaparullina, E., and Trotsenko, Y. (2014) The Family Methylophilaceae.
751 In, *The Prokaryotes*. Springer Berlin Heidelberg, Berlin, Heidelberg, pp. 869–
752 880.

753 Dorrepaal, E., Toet, S., van Logtestijn, R.S.P., Swart, E., van de Weg, M.J.,
754 Callaghan, T. V., and Aerts, R. (2009) Carbon respiration from subsurface peat
755 accelerated by climate warming in the subarctic. *Nature* **460**: 616–619.
756 Durno, W.E., Hanson, N.W., Konwar, K.M., and Hallam, S.J. (2013) Expanding the
757 boundaries of local similarity analysis. *BMC Genomics* **14 Suppl 1**: S3.
758 Edgar, R.C. (2010) Search and clustering orders of magnitude faster than BLAST.
759 *Bioinformatics* **26**: 2460–2461.
760 Embree, M., Nagarajan, H., Movahedi, N., Chitsaz, H., and Zengler, K. (2014)
761 Single-cell genome and metatranscriptome sequencing reveal metabolic
762 interactions of an alkane-degrading methanogenic community. *ISME J.* **8**: 757–
763 767.
764 Faith, D.P. (2006) The role of the phylogenetic diversity measure, PD, in bio-
765 informatics: getting the definition right. *Evol. Bioinform. Online* **2**: 277–83.
766 Faust, K. and Raes, J. (2012) Microbial interactions: from networks to models. *Nat.*
767 *Rev. Microbiol.* **10**: 538–50.
768 Faust, K., Sathirapongsasuti, J.F., Izard, J., Segata, N., Gevers, D., Raes, J., and
769 Huttenhower, C. (2012) Microbial co-occurrence relationships in the human
770 microbiome. *PLoS Comput. Biol.* **8**: e1002606.
771 Fisher, R.A., Corbet, A.S., and Williams, C.B. (1943) The Relation Between the
772 Number of Species and the Number of Individuals in a Random Sample of an
773 Animal Population. *J. Anim. Ecol.* **12**: 42–58.
774 Foster, J. a, Krone, S.M., and Forney, L.J. (2008) Application of ecological network
775 theory to the human microbiome. *Interdiscip. Perspect. Infect. Dis.* **2008**:
776 839501.
777 Freeman, C., Ostle, N.J., Fenner, N., and Kang, H. (2004) A regulatory role for
778 phenol oxidase during decomposition in peatlands. *Soil Biol. Biochem.* **36**:
779 1663–1667.
780 Friedman, J. and Alm, E.J. (2012) Inferring correlation networks from genomic

781 survey data. *PLoS Comput. Biol.* **8**: e1002687.

782 Fronzek, S., Carter, T.R., Räisänen, J., Ruokolainen, L., and Luoto, M. (2010)
783 Applying probabilistic projections of climate change with impact models: a case
784 study for sub-arctic palsa mires in Fennoscandia. *Clim. Change* **99**: 515–534.

785 Galand, P.E., Fritze, H., and Yrjala, K. (2003) Microsite-dependent changes in
786 methanogenic populations in a boreal oligotrophic fen. *Environ. Microbiol.* **5**:
787 1133–1143.

788 Giraudoux, P. (2012) pgirmess: Data analysis in ecology. R package version 1.5.6.

789 Goberna, M., García, C., and Verdú, M. (2014) A role for biotic filtering in driving
790 phylogenetic clustering in soil bacterial communities. *Glob. Ecol. Biogeogr.* **23**:
791 1346–1355.

792 Goberna, M. and Verdú, M. (2016) Predicting microbial traits with phylogenies. *ISME*
793 *J.* **10**: 959–967.

794 Godin, A., McLaughlin, J.W., Webster, K.L., Packalen, M., and Basiliko, N. (2012)
795 Methane and methanogen community dynamics across a boreal peatland
796 nutrient gradient. *Soil Biol. Biochem.* **48**: 96–105.

797 Gotelli, N.J. (2000) Null model analysis of species co-occurrence patterns. **81**: 2606–
798 2621.

799 Gurney, S.D. (2001) Aspects of the genesis, geomorphology and terminology of
800 palsas: perennial cryogenic mounds. *Prog. Phys. Geogr.* **25**: 249–260.

801 Hayes, D.J., Kicklighter, D.W., McGuire, A.D., Chen, M., Zhuang, Q., Yuan, F., et al.
802 (2014) The impacts of recent permafrost thaw on land–atmosphere greenhouse
803 gas exchange. *Environ. Res. Lett.* **9**: 45005.

804 Hedlund, B.P. (2010) Phylum Verrucomicrobia phyl. n. In, *Bergey's Manual® of*
805 *Systematic Bacteriology*. Springer New York, New York, NY, pp. 795–841.

806 Heip, C., Hill, M.O., Pielou, E.C., and Sheldon, A.L. (1974) A New Index Measuring
807 Evenness. *J. Mar. Biol. Assoc. United Kingdom* **54**: 555.

808 Hicks Pries, C.E., Schuur, E.A.G., and Crummer, K.G. (2013) Thawing permafrost

809 increases old soil and autotrophic respiration in tundra: partitioning ecosystem
810 respiration using δ(13) C and ∆(14) C. *Glob. Chang. Biol.* **19**: 649–61.
811 Hobbie, S.E., Schimel, J.P., Trumbore, S.E., and Randerson, J.R. (2000) Controls
812 over carbon storage and turnover in high-latitude soils. *Glob. Chang. Biol.* **6**:
813 196–210.
814 Hodgkins, S.B., Tfaily, M.M., McCalley, C.K., Logan, T. a, Crill, P.M., Saleska, S.R., et
815 al. (2014) Changes in peat chemistry associated with permafrost thaw increase
816 greenhouse gas production. *Proc. Natl. Acad. Sci. U. S. A.* **111**: 5819–5824.
817 Horner-Devine, M.C. and Bohannan, B.J.M. (2006) Phylogenetic clustering and
818 overdispersion in bacterial communities. *Ecology* **87**: S100–S108.
819 Huson, D.H. and Scornavacca, C. (2012) Dendroscope 3: an interactive tool for
820 rooted phylogenetic trees and networks. *Syst. Biol.* **61**: 1061–7.
821 Jackowicz-Korczyński, M., Christensen, T.R., Bäckstrand, K., Crill, P.M., Friborg, T.,
822 Mastepanov, M., and Ström, L. (2010) Annual cycle of methane emission from a
823 subarctic peatland. *J. Geophys. Res.* **115**: 1–10.
824 Johansson, M. and Åkerman, J.H. (2008) Thawing Permafrost and Thicker Active
825 Layers in Sub-arctic Sweden. *Permafr. Periglac. Process.* **19**: 279–292.
826 Johansson, T., Malmer, N., Crill, P.M., Friborg, T., Åkerman, J.H., Mastepanov, M., et
827 al. (2006) Decadal vegetation changes in a northern peatland, greenhouse gas
828 fluxes and net radiative forcing. *Glob. Chang. Biol.* **12**: 2352–2369.
829 Johnson, B.D. and Hallberg, K.B. (2008) Carbon, Iron and Sulfur Metabolism in
830 Acidophilic Micro-Organisms. *Adv. Microb. Physiol.* **54**: 201–255.
831 Jones, M.C., Harden, J., O'Donnell, J., Manies, K., Jorgenson, T., Treat, C., and
832 Ewing, S. (2016) Rapid carbon loss and slow recovery following permafrost
833 thaw in boreal peatlands. *Glob. Chang. Biol.*
834 Jones, R.T., Robeson, M.S., Lauber, C.L., Hamady, M., Knight, R., and Fierer, N.
835 (2009) A comprehensive survey of soil acidobacterial diversity using
836 pyrosequencing and clone library analyses. *ISME J.* **3**: 442–453.

837 Kämpfer, P. (2010) Actinobacteria. In, *Handbook of Hydrocarbon and Lipid*
838 *Microbiology*. Springer Berlin Heidelberg, Berlin, Heidelberg, pp. 1819–1838.
839 Kembel, S.W., Cowan, P.D., Helmus, M.R., Cornwell, W.K., Morlon, H., Ackerly, D.D.,
840 et al. (2010) Picante: R tools for integrating phylogenies and ecology.
841 *Bioinformatics* **26**: 1463–4.
842 Kim, Y. and Liesack, W. (2015) Differential assemblage of functional units in paddy
843 soil microbiomes. *PLoS One* **10**:.
844 King, A.J., Farrer, E.C., Suding, K.N., and Schmidt, S.K. (2012) Co-occurrence
845 patterns of plants and soil bacteria in the high-alpine subnival zone track
846 environmental harshness. *Front. Microbiol.* **3**: 347.
847 Kokfelt, U., Reuss, N., Struyf, E., Sonesson, M., Rundgren, M., Skog, G., et al.
848 (2010) Wetland development, permafrost history and nutrient cycling inferred
849 from late Holocene peat and lake sediment records in subarctic Sweden. *J.*
850 *Paleolimnol.* **44**: 327–342.
851 Kotsyurbenko, O.R., Friedrich, M.W., Simankova, M. V, Nozhevnikova, a N.,
852 Golyshin, P.N., Timmis, K.N., and Conrad, R. (2007) Shift from acetoclastic to
853 H2-dependent methanogenesis in a west Siberian peat bog at low pH values
854 and isolation of an acidophilic Methanobacterium strain. *Appl. Environ.*
855 *Microbiol.* **73**: 2344–8.
856 Kraft, N.J.B.N., Cornwell, W.K.W., Webb, C.C.O., and Ackerly, D.D. (2007) Trait
857 evolution, community assembly, and the phylogenetic structure of ecological
858 communities. *Am. Nat.* **170**: 271–283.
859 Krieg, N.R., Staley, J.T., Brown, D.R., Hedlund, B.P., Paster, B.J., Ward, N.L., et al.
860 (2010) Bergey's Volume 4 Bacteroidetes, Acidobacteria, Spirochaetes etc.
861 Kulichevskaya, I.S., Kostina, L.A., Valášková, V., Rijpstra, W.I.C., Sinninghe Damsté,
862 J.S., de Boer, W., and Dedysh, S.N. (2012) Acidicapsa borealis gen. nov., sp.
863 nov. and Acidicapsa ligni sp. nov., subdivision 1 Acidobacteria from Sphagnum
864 peat and decaying wood. *Int. J. Syst. Evol. Microbiol.* **62**: 1512–1520.

865 Lazar, C.S., Baker, B.J., Seitz, K., Hyde, A.S., Dick, G.J., Hinrichs, K.U., and Teske,
866 A.P. (2016) Genomic evidence for distinct carbon substrate preferences and
867 ecological niches of Bathyarchaeota in estuarine sediments. *Environ. Microbiol.*
868 **18**: 1200–1211.
869 Liebner, S., Ganzert, L., Kiss, A., Yang, S., Wagner, D., and Svenning, M.M. (2015)
870 Shifts in methanogenic community composition and methane fluxes along the
871 degradation of discontinuous permafrost. *Front. Microbiol.* **6**: 1–10.
872 Lin, X., Green, S., Tfaily, M.M., Prakash, O., Konstantinidis, K.T., Corbett, J.E., et al.
873 (2012) Microbial community structure and activity linked to contrasting
874 biogeochemical gradients in bog and fen environments of the Glacial Lake
875 Agassiz Peatland. *Appl. Environ. Microbiol.* **78**: 7023–7031.
876 Lin, X., Tfaily, M.M., Green, S.J., Steinweg, J.M., Chanton, P., Imvittaya, A., et al.
877 (2014) Microbial metabolic potential for carbon degradation and nutrient
878 (nitrogen and phosphorus) acquisition in an ombrotrophic peatland. *Appl.*
879 *Environ. Microbiol.* **80**: 3531–40.
880 Lü, Z. and Lu, Y. (2012) Methanocella conradii sp. nov., a Thermophilic, Obligate
881 Hydrogenotrophic Methanogen, Isolated from Chinese Rice Field Soil. *PLoS*
882 *One* **7**: e35279.
883 Lyu, Z. and Lu, Y. (2015) Comparative genomics of three Methanocellales strains
884 reveal novel taxonomic and metabolic features. *Environ. Microbiol. Rep.* **7**: 526–
885 537.
886 Mack, M.C., Bret-Harte, M.S., Hollingsworth, T.N., Jandt, R.R., Schuur, E.A.G.,
887 Shaver, G.R., and Verbyla, D.L. (2011) Carbon loss from an unprecedented
888 Arctic tundra wildfire. *Nature* **475**: 489–92.
889 Malmer, N., Johansson, T., Olsrud, M., and Christensen, T.R. (2005) Vegetation,
890 climatic changes and net carbon sequestration in a North-Scandinavian
891 subarctic mire over 30 years. *Glob. Chang. Biol.* **11**: 1895–1909.
892 Martiny, A.C., Treseder, K., and Pusch, G. (2013) Phylogenetic conservatism of

functional traits in microorganisms. *ISME J.* **7**: 830–8.

Masing, V., Botch, M., and Lääne laid, a. (2009) Mires of the former Soviet Union. *Wetl. Ecol. Manag.* **18**: 397–433.

Matsuo, H., Kudo, C., Li, J., and Tonouchi, A. (2016) Acidicapsa acidisoli sp. nov. from the acidic soil of a deciduous forest. *Int. J. Syst. Evol. Microbiol.*

Mayfield, M.M. and Levine, J.M. (2010) Opposing effects of competitive exclusion on the phylogenetic structure of communities. *Ecol. Lett.* **13**: 1085–93.

McCalley, C.K., Woodcroft, B.J., Hodgkins, S.B., Wehr, R.A., Kim, E.-H., Mondav, R., et al. (2014) Methane dynamics regulated by microbial community response to permafrost thaw. *Nature* **514**: 478–481.

McDonald, D., Price, M.N., Goodrich, J., Nawrocki, E.P., DeSantis, T.Z., Probst, A., et al. (2012) An improved Greengenes taxonomy with explicit ranks for ecological and evolutionary analyses of bacteria and archaea. *ISME J.* **6**: 610–8.

McGuire, A.D., Macdonald, R.W., Schuur, E.A.G., Harden, J.W., Kuhry, P., Hayes, D.J., et al. (2010) The carbon budget of the northern cryosphere region. *Curr. Opin. Environ. Sustain.* **2**: 231–236.

Mondav, R., Woodcroft, B.J., Kim, E.-H., McCalley, C.K., Hodgkins, S.B., Crill, P.M., et al. (2014) Discovery of a novel methanogen prevalent in thawing permafrost. *Nat. Commun.* **5**: 1–7.

Natali, S.M., Schuur, E.A.G., Trucco, C., Hicks Pries, C.E., Crummer, K.G., and Baron Lopez, A.F. (2011) Effects of experimental warming of air, soil and permafrost on carbon balance in Alaskan tundra. *Glob. Chang. Biol.* **17**: 1394–1407.

Nazaries, L., Murrell, J.C., Millard, P., Baggs, L., and Singh, B.K. (2013) Methane, microbes and models: fundamental understanding of the soil methane cycle for future predictions. *Environ. Microbiol.* **15**: 2395–2417.

Nilsson, A. (2006) Limnological responses to late Holocene permafrost dynamics at the Stordalen mire , Abisko , northern Sweden Examensarbeten i Geologi vid.

921 *Science (80-.).*

922 Nilsson, M. and Bohlin, E. (1993) Methane and carbon dioxide concentrations in
923 bogs and fens - with special reference to the effects of the botanical composition
924 of the peat. *Br. Ecol. Soc.* **81**: 615–625.

925 O'Donnell, J.A., Jorgenson, M.T., Harden, J.W., McGuire, A.D., Kanevskiy, M.Z., and
926 Wickland, K.P. (2012) The Effects of Permafrost Thaw on Soil Hydrologic,
927 Thermal, and Carbon Dynamics in an Alaskan Peatland. *Ecosystems* **15**: 213–
928 229.

929 Olefeldt, D., Turetsky, M.R., Crill, P.M., and Mcguire, A.D. (2013) Environmental and
930 physical controls on northern terrestrial methane emissions across permafrost
931 zones. *Glob. Chang. Biol.* **19**: 589–603.

932 Oren, A. (2014a) The Family Methanobacteriaceae. In, *The Prokaryotes*. Springer
933 Berlin Heidelberg, Berlin, Heidelberg, pp. 165–193.

934 Oren, A. (2014b) The Family Methanoregulaceae. In, *The Prokaryotes*. Springer
935 Berlin Heidelberg, Berlin, Heidelberg, pp. 253–258.

936 Oren, A. (2014c) The Family Methanosarcinaceae. In, *The Prokaryotes*. Springer
937 Berlin Heidelberg, Berlin, Heidelberg, pp. 259–281.

938 Osterkamp, T.E., Jorgenson, M.T., Schuur, E.A.G., Shur, Y.L., Kanevskiy, M.Z., and
939 Vogel, J.G. (2009) Physical and Ecological Changes Associated with Warming
940 Permafrost and Thermokarst in Interior Alaska. *Permafr. Periglac. Process.* **20**:
941 235–256.

942 Pankratov, T.A., Kirsanova, L.A., Kaparullina, E.N., Kevbrin, V. V., and Dedysh, S.N.
943 (2012) Telmatobacter bradus gen. nov., sp. nov., a cellulolytic facultative
944 anaerobe from subdivision 1 of the Acidobacteria, and emended description of
945 Acidobacterium capsulatum Kishimoto et al. 1991. *Int. J. Syst. Evol. Microbiol.*
946 **62**: 430–437.

947 Parviainen, M. and Luoto, M. (2007) Climate envelopes of mire complex types in
948 Fennoscandia. *Geography* **89**: 137–151.

949 Paul, K., Nonoh, J.O., Mikulski, L., and Brune, A. (2012) “Methanoplasmatales,”
950 Thermoplasmatales-related archaea in termite guts and other environments, are
951 the seventh order of methanogens. *Appl. Environ. Microbiol.* **78**: 8245–53.
952 Payette, S., Delwaide, A., Caccianiga, M., and Beauchemin, M. (2004) Accelerated
953 thawing of subarctic peatland permafrost over the last 50 years. *Geophys. Res.*
954 *Lett.* **31**: 1–4.
955 Price, M.N., Dehal, P.S., and Arkin, A.P. (2010) FastTree 2--approximately maximum-
956 likelihood trees for large alignments. *PLoS One* **5**: e9490.
957 Putkinen, A., Larmola, T., Tuomivirta, T., Siljanen, H.M.P., Bodrossy, L., Tuittila, E.-S.,
958 and Fritze, H. (2012) Water dispersal of methanotrophic bacteria maintains
959 functional methane oxidation in sphagnum mosses. *Front. Microbiol.* **3**: 15.
960 Quast, C., Pruesse, E., Yilmaz, P., Gerken, J., Schweer, T., Yarza, P., et al. (2013)
961 The SILVA ribosomal RNA gene database project: improved data processing
962 and web-based tools. *Nucleic Acids Res.* **41**: D590-6.
963 Quiroga, M.V., Valverde, A., Mataloni, G., and Cowan, D. (2015) Understanding
964 diversity patterns in bacterioplankton communities from a sub-Antarctic
965 peatland. *Environ. Microbiol. Rep.* 1–7.
966 Railton, J.B. and Sparling, J.H. (1973) Preliminary studies on the ecology of palsa
967 mounds in northern Ontario. *J. Bot.* **51**: 1037–1044.
968 Rundqvist, S., Hedenås, H., Sandström, A., Emanuelsson, U., Eriksson, H.,
969 Jonasson, C., and Callaghan, T. V (2011) Tree and shrub expansion over the
970 past 34 years at the tree-line near Abisko, Sweden. *Ambio* **40**: 683–92.
971 Rydén, B.E., Fors, L., and Kostov, L. (1980) Physical Properties of the Tundra Soil-
972 Water System at Stordalen , Abisko. *Ecol. Bull.* **30**: 27–54.
973 Sakai, S., Conrad, R., Liesack, W., and Imachi, H. (2010) Methanocella arvoryzae
974 sp. nov., a hydrogenotrophic methanogen isolated from rice field soil. *Int. J.*
975 *Syst. Evol. Microbiol.* **60**: 2918–23.
976 Schuur, E.A.G., McGuire, A.D., Schädel, C., Grosse, G., Harden, J.W., Hayes, D.J.,

et al. (2015) Climate change and the permafrost carbon feedback. *Nature* **520**: 171–179.

Seppälä, M. (2011) Synthesis of studies of palsa formation underlining the importance of local environmental and physical characteristics. *Quat. Res.* **75**: 366–370.

Serkebaeva, Y.M., Kim, Y., Liesack, W., and Dedysh, S.N. (2013) Pyrosequencing-Based Assessment of the Bacteria Diversity in Surface and Subsurface Peat Layers of a Northern Wetland, with Focus on Poorly Studied Phyla and Candidate Divisions. *PLoS One* **8**: e63994.

Shade, A., Peter, H., Allison, S.D., Baho, D.L., Berga, M., Bürgmann, H., et al. (2012) Fundamentals of microbial community resistance and resilience. *Front. Microbiol.* **3**: 417.

Shannon, C.E. and Weaver, W. (1949) A mathematical theory of communication University of Illinois Press, Urbana.

Sharp, C.E., den Camp, H.J.M.O., Tamas, I., and Dunfield, P.F. (2013) Unusual Members of the PVC Superphylum: The Methanotrophic Verrucomicrobia Genus “Methylacidiphilum.” In, *Planctomycetes: Cell Structure, Origins and Biology*. Humana Press, Totowa, NJ, pp. 211–227.

Shur, Y.L. and Jorgenson, M.T. (2007) Patterns of Permafrost Formation and Degradation in Relation to Climate and Ecosystems. *Permafr. Periglac. Process.* **18**: 7–19.

Singh, B.K., Quince, C., Macdonald, C. a, Khachane, A., Thomas, N., Al-Soud, W.A., et al. (2014) Loss of microbial diversity in soils is coincident with reductions in some specialized functions. *Environ. Microbiol.* **16**: 2408–2420.

Smith, K.S. and Ingram-Smith, C. (2007) Methanosaeta, the forgotten methanogen?

Sollid, J.L. and Sørbel, L. (1998) Palsa Bogs as a Climate Indicator: Examples from Dovrefjell, Southern Norway. *Ambio* **27**: 287–291.

Stackebrandt, E. (2014) The Family Acidimicrobiaceae. In, *The Prokaryotes:*

Actinobacteria., pp. 1–1061.

Stegen, J.C., Lin, X., Fredrickson, J.K., Chen, X., Kennedy, D.W., Murray, C.J., et al. (2013) Quantifying community assembly processes and identifying features that impose them. *ISME J.* **7**: 2069–2079.

Stegen, J.J.C., Lin, X., Konopka, A.E.A., and Fredrickson, J.K.J. (2012) Stochastic and deterministic assembly processes in subsurface microbial communities. *ISME J.* **6**: 1653–64.

Turetsky, M.R., Wieder, R.K., Vitt, D.H., Evans, R.J., and Scott, K.D. (2007) The disappearance of relict permafrost in boreal north America: Effects on peatland carbon storage and fluxes. *Glob. Chang. Biol.* **13**: 1922–1934.

Tveit, A., Schwacke, R., Svenning, M.M., and Urich, T. (2013) Organic carbon transformations in high-Arctic peat soils: key functions and microorganisms. *ISME J.* **7**: 299–311.

Venail, P. a. and Vives, M.J. (2013) Phylogenetic distance and species richness interactively affect the productivity of bacterial communities. *Ecology* **94**: 2529–2536.

Wagner, D. and Liebner, S. (2009) Global Warming and Carbon Dynamics in Permafrost Soils : Methane Production and Oxidation. In, Margesin,R. (ed), *Soil Biology*, Soil Biology. Springer, Berlin, pp. 219–236.

Ward, N.L., Challacombe, J.F., Janssen, P.H., Henrissat, B., Coutinho, P.M., Wu, M., et al. (2009) Three genomes from the phylum Acidobacteria provide insight into the lifestyles of these microorganisms in soils. *Appl. Environ. Microbiol.* **75**: 2046–56.

Webb, C.O., Ackerly, D.D., McPeek, M.A., and Donoghue, M.J. (2002) PHYLOGENIES AND COMMUNITY ECOLOGY. *Annu. Rev. Ecol. Syst.* **33**: 475–505.

Weiss, S., Van Treuren, W., Lozupone, C., Faust, K., Friedman, J., Deng, Y., et al. (2016) Correlation detection strategies in microbial data sets vary widely in

1033 sensitivity and precision. *Isme J* 1–13.

1034 Werner, J.J., Knights, D., Garcia, M.L., Scalfone, N.B., Smith, S., Yarasheski, K., et
1035 al. (2011) Bacterial community structures are unique and resilient in full-scale
1036 bioenergy systems. *Proc. Natl. Acad. Sci. U. S. A.* **108**: 4158–63.

1037 Whitfeld, T.J.S., Kress, W.J., Erickson, D.L., and Weiblen, G.D. (2012) Change in
1038 community phylogenetic structure during tropical forest succession: evidence
1039 from New Guinea. *Ecography (Cop.).* **35**: 821–830.

1040 Yang, S.J., Kang, I., and Cho, J.C. (2016) Expansion of Cultured Bacterial Diversity
1041 by Large-Scale Dilution-to-Extinction Culturing from a Single Seawater Sample.
1042 *Microb. Ecol.* **71**: 29–43.

1043 Yavitt, J.B., Yashiro, E., Cadillo-Quiroz, H., and Zinder, S.H. (2011) Methanogen
1044 diversity and community composition in peatlands of the central to northern
1045 Appalachian Mountain region, North America. *Biogeochemistry* **109**: 117–131.

1046 Zoltai, S.C. (1993) Cyclic Development of Permafrost in the Peatlands of
1047 Northwestern Canada. *Arct. Alp. Res.* **25**: 240–246.

1048

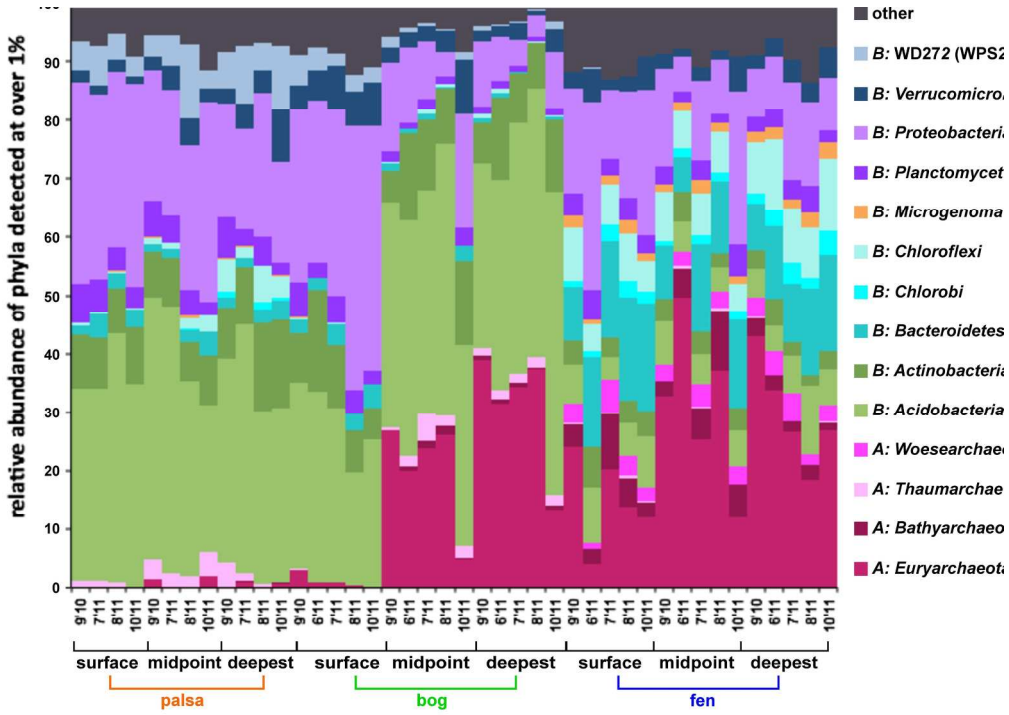

Fig 1 Mean relative abundance of phyla present at over 1 %. Samples grouped by site, then depth, then date. Date is marked along the horizontal axis as m'yy.

210x148mm (300 x 300 DPI)

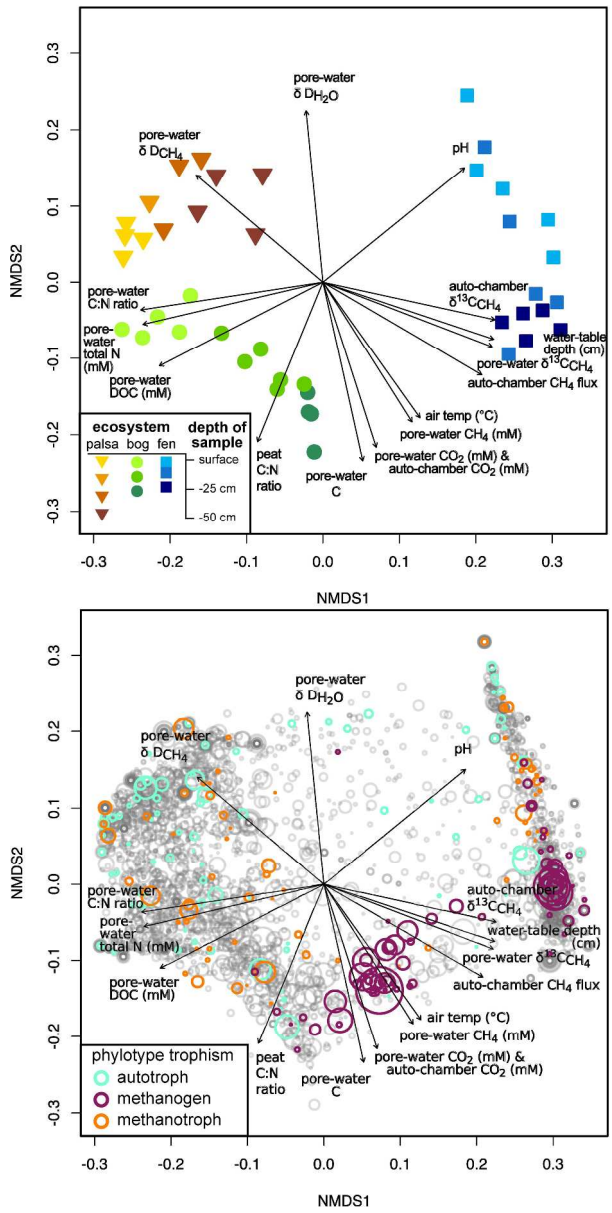

Fig 2 NMDS analysis of sample dissimilarity in community phylotype space, and environmental correlates (Stress = 0.0818, r2 = 0.993). a) The clustering of sites based on their community composition; sites are distinguished by shape and colored to show depth of sample; b) The relative positional contribution of phylotypes to this clustering, with phylotypes plotted as circles with diameter scaled to the log of the mean abundance, and colored to show putative C-cycle metabolism. Plotted vectors on a) & b) are measured environmental variables that had significant correlation to differences in assemblage composition ($p < 0.01$), with the terminal arrow indicating the direction of strongest change without reference to sign (+ or -).

285x572mm (300 x 300 DPI)

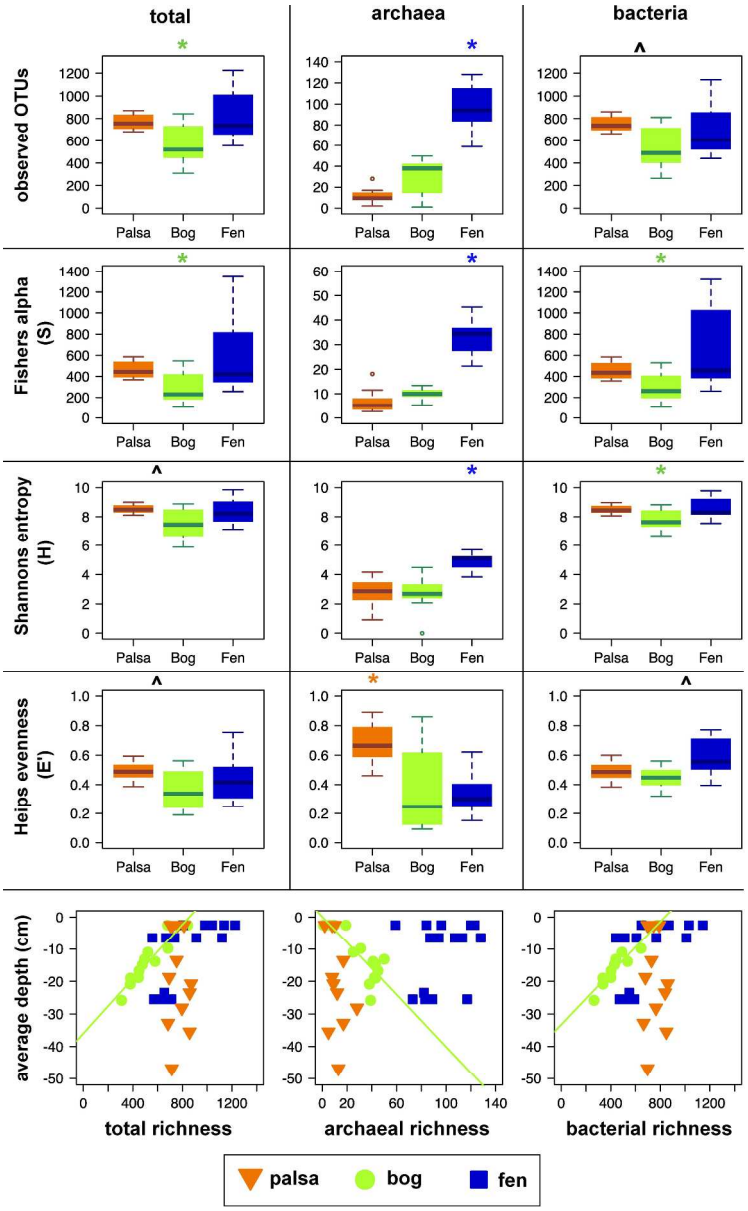

Fig 3 By-site comparison of alpha diversity metrics. a) The distribution of observed richness (top), Fisher's alpha-S (2nd from top), Shannon's entropy-H (2nd from bottom), Heip's evenness (bottom), on all 97 % OTUs (left), archaeal OTUs (middle) and bacterial OTUs (right) in combined normalized (N=2000) samples. Significant differences were measured by Kruskal-Wallis post-hoc test (* $p < 0.001$, where * designates a site significantly different from the other two sites and ^ designates a significant difference between the two adjacent sites only)). b) The distribution of OTU richness with sample depth for all OTUs (left), archaeal OTUs (centre), bacterial OTUs (right). Green trend lines show the correlations between richness and depth of sample in the bog site.

301x488mm (300 x 300 DPI)

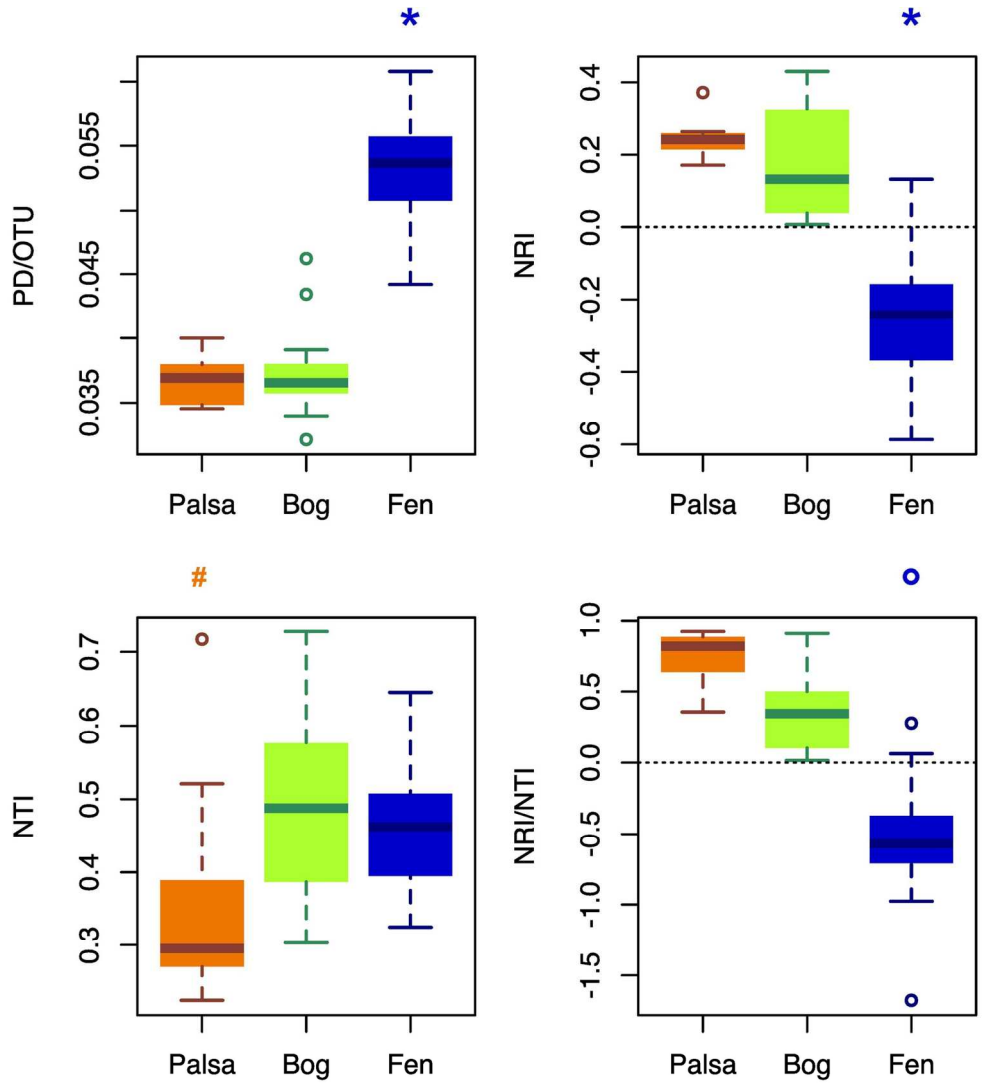

Fig 4 By-site comparison of phylogenetic diversity. topleft: faiths phylogenetic distance per OTU (PD/OTU); bottom left: Nearest taxon index (NTI); top right: Net relatedness Index (NRI), bottom right: NRI/NTI ratio.

147x167mm (300 x 300 DPI)

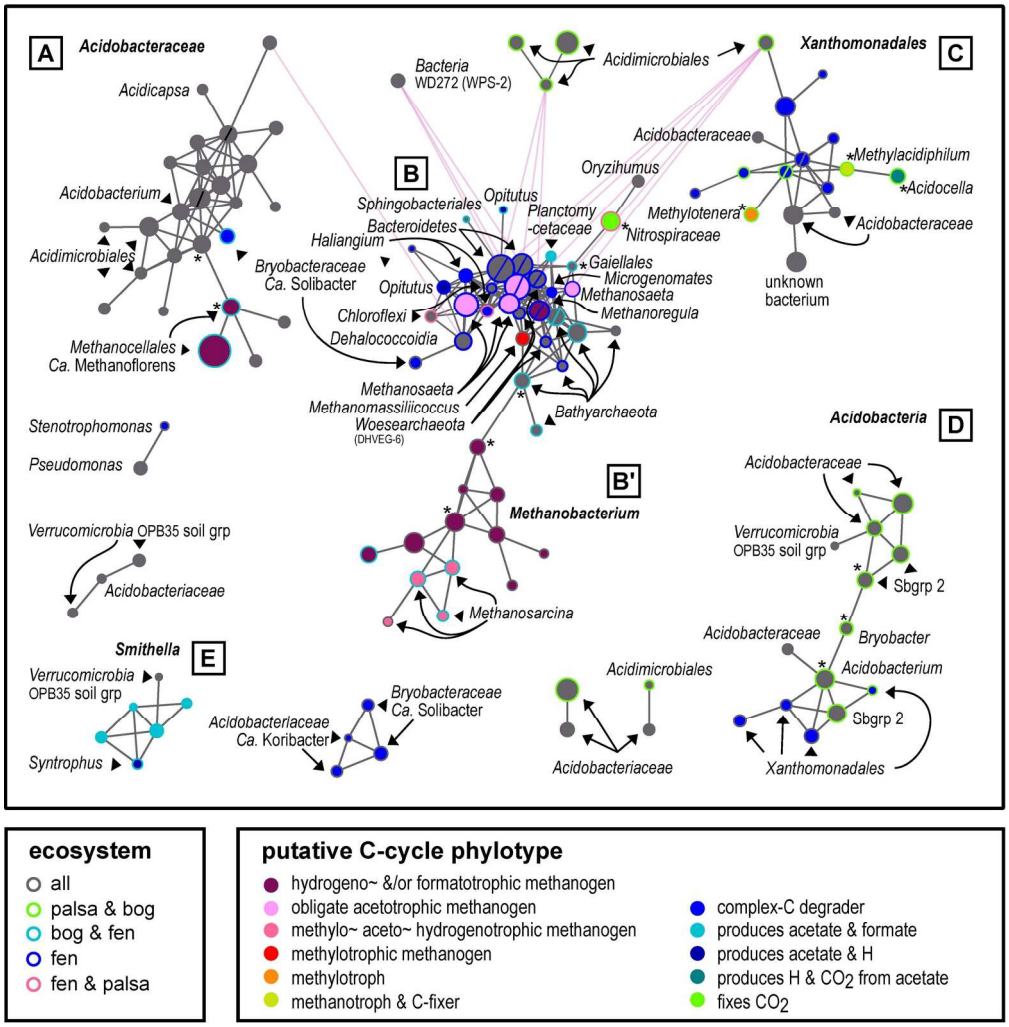

ecosystem
- all
- palsa & bog
- bog & fen
- fen
- fen & palsa

putative C-cycle phylotype
- hydrogeno~ &/or formatotrophic methanogen
- obligate acetotrophic methanogen
- methylo~ aceto~ hydrogenotrophic methanogen
- methylotrophic methanogen
- methylotroph
- methanotroph & C-fixer
- complex-C degrader
- produces acetate & formate
- produces acetate & H
- produces H & CO_2 from acetate
- fixes CO_2

Fig 5 Network of phylotypes present in at least 15 samples with significant pairwise correlation. Circles indicate individual OTUs; circle diameter is a function of the log of the mean abundance. Circle colour denotes phylogenetically-inferred metabolism, and the colour of the outline denotes ecosystem presence. Circles with * are putative keystones and those with a / across the middle are putative hubs. Grey edges indicate co-occurrence, while pink edges indicate mutual-exclusion.

181x184mm (300 x 300 DPI)